AIMS Mathematics, 7(4): 5117–5132.
DOI: 10.3934/math.2022285
Received: 13 September 2021
Revised: 15 December 2021
Accepted: 23 December 2021
Published: 31 December 2021

http://www.aimspress.com/journal/Math

Research article

Dynamical behavior and control of a new hyperchaotic Hamiltonian system

Junhong Li and Ning Cui*

School of Mathematics and Statistics, Hanshan Normal University, Chaozhou, Guangdong, 521041, China

* **Correspondence:** Email: cnmath80@163.com.

Abstract: In this paper, we firstly formulate a new hyperchaotic Hamiltonian system and demonstrate the existence of multi-equilibrium points in the system. The characteristics of equilibrium points, Lyapunov exponents and Poincaré sections are studied. Secondly, we investigate the complex dynamical behaviors of the system under holonomic constraint and nonholonomic constraint, respectively. The results show that the hyperchaotic system can generated by introducing constraint. Additionally, the hyperchaos control of the system is achieved by applying linear feedback control. The numerical simulations are carried out in order to analyze the complex phenomena of the systems.

Keywords: Hamiltonian system; hyperchaos; constraint; hyperchaos control
Mathematics Subject Classification: 34K18, 34H10, 65P20

1. Introduction

As a kind of important model, Hamiltonian system is widely used in many fields [1–7]. And the chaotic behaviors of Hamiltonian systems have attracted many scientists and many remarkable research results are obtained. Based on energy analysis of a Sprott-A system, H. Jia and his cooperators formulate a new four-dimension chaotic Hamiltonian system. Then the chaotic characteristic of the 4-D system and the existence of coexisting hidden attractors are studied by numerical analysis and field programmable gate array (FPGA) implementation [8]. The Sprott-A system is reported by Sprott in 1994, which is a algebraically simple three-dimensional chaotic system [9]. The chaotic behaviors of a paradigmatic low-dimensional Hamiltonian system subjected to different scenarios of parameter drifts of non-negligible rates are investigated in [10]. In addition, similar studies were carried out in [11–13]. Compared to chaos, hyperchaos is more complex and has stronger randomness and unpredictability. Thus, hyperchaos has great potential applications. For example, hyperchaos could help us build better quantum computer [14]. Therefore, we constructed a new hyperchaotic Hamiltonian system. The rich dynamical behaviors of the system with holonomic

constraint and nonholonomic constraint, and hyperchaos control are investigated.

The organization of this paper is as follows. In Section 2, we formulate a six-dimension hyperchaotic Hamiltonian system. The invariance, equilibrium points and their linear stability, and hyperchaotic behaviors of the system are analyzed. In Section 3, we present a holonomic constrained system and a nonholonomic constrained system, respectively. By using the method of [15], the explicit equations for constrained systems are obtained. The influences of constrained condition on the hyperchaotic behaviors of the Hamiltonian system are investigated. In Section 4, based on feedback control, how to control the hyperchaotic behaviors of the Hamiltonian system and holonomic system are studied. The conclusions are summarized in Section 5.

2. Hyperchaotic Hamiltonian system

In this section, we assume that the Hamiltonian system is described by a function

$$H(\boldsymbol{q},\boldsymbol{p},t)=\frac{p_1^2+p_2^2+p_3^2-\theta q_1^2-\theta q_2^2-\theta q_3^2}{2}+\frac{\beta(q_1^4+q_2^4+q_3^4)}{4}+\eta q_1(q_3+q_2-\frac{\eta q_1}{2}), \tag{2.1}$$

here $\boldsymbol{q}=(q_1,q_2,q_3)$ is the generalized coordinate, $\boldsymbol{p}=(p_1,p_2,p_3)$ is the canonical momentum and t denotes time. Then, we obtain the Hamiltonian system as follows:

$$\begin{cases} \dot{q}_1=p_1,\\ \dot{q}_2=p_2,\\ \dot{q}_3=p_3,\\ \dot{p}_1=-\beta q_1^3+(\eta^2+\theta)q_1-\eta(q_2+q_3),\\ \dot{p}_2=-\beta q_2^3+\theta q_2-\eta q_1,\\ \dot{p}_3=-\beta q_3^3+\theta q_3-\eta q_1, \end{cases} \tag{2.2}$$

where, θ,β,η are positive parameters. The dot expresses the derivative with respect to t.

Obviously, the system (2.2) is invariant for the coordinate transformation

$$(q_1,q_2,q_3,p_1,p_2,p_3)\to(-q_1,-q_2,-q_3,-p_1,-p_2,-p_3),$$

thus it is symmetric with respect to the origin. For arbitrary equilibrium point $\mathbf{E}=(q_1,q_2,q_3,p_1,p_2,p_3)$ of (2.2), the Jacobian matrix is

$$\begin{bmatrix} O & \boldsymbol{I}_3\\ J_3 & O \end{bmatrix},$$

where $\boldsymbol{I}_3$ denotes third order identity matrix and

$$J_3=\begin{bmatrix} -3\beta q_1^2+\eta^2+\theta & -\eta & -\eta\\ -\eta & -3\beta {q_2}^2+\theta & 0\\ -\eta & 0 & -3\beta {q_3}^2+\theta \end{bmatrix}.$$

Correspondingly, the characteristic equation at $\mathbf{E}$ is as follows:

$$f(\lambda)=\lambda^6-tr\,(J_3)\,\lambda^4+\tau\,\lambda^2-|J_3|\,, \tag{2.3}$$

where

$$\tau = (9\,{q_1}^2{q_2}^2 + 9\,{q_1}^2{q_3}^2 + 9\,{q_2}^2{q_3}^2)\beta^2 + (-3\,(\eta^2+\theta){q_2}^2 - 6\,{q_1}^2\theta - 3\,(\eta^2+\theta){q_3}^2 - 3\,{q_2}^2\theta$$
$$-3\,\theta\,{q_3}^2)\beta + 2\,(\eta^2+\theta)\theta + \theta^2 - 2\,\eta^2.$$

It is easy to visualize that the system (2.2) always has the equilibrium point $\mathbf{E}_0 = (0,0,0,0,0,0)$, the characteristic equation of Jacobian matrix is

$$\lambda^6 + \left(-\eta^2 - 3\,\theta\right)\lambda^4 + \left(2\,\left(\eta^2+\theta\right)\theta + \theta^2 - 2\,\eta^2\right)\lambda^2 - \theta^2\left(\eta^2+\theta\right) + 2\,\eta^2\theta. \tag{2.4}$$

In the following, similar to [16], we investigate the stability of $\mathbf{E}_0$ by discussing the coefficients of characteristic polynomial at different conditions. When $\eta^2\theta + \theta^2 \geq 2\eta^2$, the roots of the characteristic equation are

$$\lambda_{1,2} = \pm\sqrt{\theta},\ \lambda_{3,4} = \pm\frac{\sqrt{2\,\eta^2+2\,\sqrt{\eta^4+8\,\eta^2}+4\,\theta}}{2},\ \lambda_{5,6} = \pm\frac{\sqrt{2\,\eta^2-2\,\sqrt{\eta^4+8\,\eta^2}+4\,\theta}}{2}.$$

When $\eta^2\theta + \theta^2 \leq 2\eta^2$, $\lambda_{5,6}$ becomes

$$\pm\frac{\sqrt{2\,\eta^2 - 2\,\sqrt{\eta^4+8\,\eta^2}+4\,\theta}}{2}i,$$

the other characteristic roots above remain unchanged. It shows that $\mathbf{E}_0$ is an unstable equilibrium point.

Next, we illustrate that the system (2.2) exist non-zero equilibrium point. Let $\dot{p}_2 = 0$, $\dot{p}_3 = 0$, we have $\beta\,{q_2}^3 - \theta\,q_2 = \beta\,{q_3}^3 - \theta\,q_3$, $(q_2 - q_3)(\beta\,{q_2}^2 + \beta\,q_2q_3 + \beta\,{q_3}^2 - \theta) = 0$, then

$$q_2 = q_3,\ {q_2}^2 + q_2q_3 + {q_3}^2 = \tfrac{\theta}{\beta}.$$

When $q_2 = q_3$, substitute $q_1 = \frac{q_2(\beta\,{q_2}^2-\theta)}{\eta}$ into $\dot{p}_1 = 0$, direct calculation shows that

$$q_2 f(q_2) = 0,\ f(q_2) = \tfrac{\beta^4{q_2}^8}{\eta^3} - \tfrac{3\beta^3\theta\,{q_2}^6}{\eta^3} + \tfrac{3\beta^2\theta^2{q_2}^4}{\eta^3} + (-\tfrac{\beta\,\theta^3}{\eta^3} + \tfrac{(\eta^2+\theta)\beta}{\eta}){q_2}^2 - \tfrac{(\eta^2+\theta)\theta}{\eta} - 2\,\eta.$$

Since

$$\lim_{q_2\to 0} f(q_2) < 0,\quad \lim_{q_2\to\infty} f(q_2) > 0,$$

it follows that $f(q_2)$ has non-zero roots. Furthermore, if $q_2 = 0$, we have $q_1 = 0$ based on $\dot{p}_2 = 0$, then we have $q_3 = 0$ based on $\dot{p}_1 = 0$. And we also obtain $q_1 = 0$, $q_2 = 0$ when $q_3 = 0$. Therefore, if q_2 and q_3 satisfy ${q_2}^2 + q_2q_3 + {q_3}^2 - \frac{\theta}{\beta} = 0$, we obtain $q_2q_3 \neq 0$. In conclusion, the system (2.2) exist non-zero equilibrium point.

To further illustrate the equilibrium points and dynamical behaviors of the system (2.2), we fix the parameters $\eta = 0.1$, $\theta = 0.5$, $\beta = 2.5$. The calculations show that the system (2.2) has twenty-seven equilibrium points, the values of equilibrium points and their corresponding characteristic root results are given in Table 1. It shows that the system (2.2) has hyperbolic equilibrium points and non-hyperbolic equilibrium points, and there exist unstable manifold and stable manifold around the equilibrium points from Table 1. Here, all the calculation results are done by Maple software. Because it does not affect the description and result of the problem, for the convenience of expression, only approximate results are given in this paper. For the other calculation results, the same process is done based on the same consideration. It has been long supposed that the existence of chaotic behavior in the microscopic motions is responsible for their equilibrium and non-equilibrium properties [17]. In addition, Lyapunov characteristic exponents have been widely employed in studying dynamical

systems, especially for measuring the exponential divergence of nearby orbits along certain directions in phase space [18, 19]. A. Wolf and his cooperators have presented a trajectory algorithm to calculate the Lyapunov exponents [20]. The basic idea of the method is to keep track of perturbations away from the trajectory in linearized phase space. And the Wolf algorithm is comparatively suitable for the analysis of experimental data [21]. So in this paper, we calculate the Lyapunov exponents using Wolf method, where the system is integrated using a fourth-order Runge Kutta method with a fixed step size equal to 0.01 [21]. And any system containing more than one positive Lyapunov exponent is defined to be hyperchaotic [22]. By computations, the Lyapunov exponents are obtained as follows:

$$LE_1 \approx 0.125, LE_2 \approx 0.067, LE_3 \approx 0.000, LE_4 \approx -0.000, LE_5 \approx -0.067, LE_6 \approx -0.125,$$

thus the system (2.2) is hyperchaotic. The spectra of Lyapunov exponents of (2.2) is given in Figure 1. It indicates that the values of Lyapunov exponents tend to stable after 40000 steps.

Table 1. The equilibrium points and their corresponding eigenvalues of system (2.2).

equilibrium points	eigenvalues of Jacobian matrix at these equilibria
$(0, 0, 0, 0, 0, 0)$	$\pm 0.7071067 \quad \pm 0.6029015 \quad \pm 0.8040582$
$(0, 0.4472135, -0.4472135, 0, 0, 0)$	$\pm i \quad \pm 1.0065440i \quad \pm 0.7232778$
$(0, -0.4472135, 0.4472135, 0, 0, 0)$	$\pm i \quad \pm 1.0065440i \quad \pm 0.7232778$
$(0.2148994, 0.4239380, 0.4239380, 0, 0, 0)$	$\pm 0.4278272 \quad \pm 0.9208291i \quad \pm 0.9313031i$
$(-0.2148994, -0.424, -0.4239380, 0, 0, 0)$	$\pm 0.4278272 \quad \pm 0.9208291i \quad \pm 0.9313031i$
$(0.3159384, 0.4114423, 0.4114423, 0, 0, 0)$	$\pm 0.4509019i \quad \pm 0.8772889i \quad \pm 0.8971908i$
$(-0.3159384, -0.4114423, -0.4114423, 0, 0, 0)$	$\pm 0.4509019i \quad \pm 0.8772889i \quad \pm 0.8971908i$
$(0.4328059, 0.0902347, 0.0902347, 0, 0, 0)$	$\pm 0.6625199 \quad \pm 0.6736186 \quad \pm 0.9538011i$
$(-0.4328059, -0.0902347, -0.0902347, 0, 0, 0)$	$\pm 0.6625199 \quad \pm 0.6736186 \quad \pm 0.9538011i$
$(0.5279016, -0.4927975, -0.4927975, 0, 0, 0)$	$\pm 1.1220833i \quad \pm 1.1495087i \quad \pm 1.2815618i$
$(-0.5279016, 0.4927975, 0.4927975, 0, 0, 0)$	$\pm 1.1220833i \quad \pm 1.1495087i \quad \pm 1.2815618i$
$(0.0934702, 0.0187268, 0.4375559, 0, 0, 0)$	$\pm 0.6100958 \quad \pm 0.7595198 \quad \pm 0.9711627i$
$(-0.0934702, -0.0187268, -0.4375559, 0, 0, 0)$	$\pm 0.6100958 \quad \pm 0.7595198 \quad \pm 0.9711627i$
$(0.3936921, 0.0814390, 0.4008976, 0, 0, 0)$	$\pm 0.6777331 \quad \pm 0.7625330i \quad \pm 0.8862569i$
$(-0.3936921, -0.0814390, -0.4008976, 0, 0, 0)$	$\pm 0.6777331 \quad \pm 0.7625330i \quad \pm 0.8862569i$
$(0.4608604, 0.3909578, -0.4876500, 0, 0, 0)$	$\pm 0.7898325i \quad \pm 1.0304795i \quad \pm 1.1519976i$
$(-0.4608604, -0.3909578, 0.4876500, 0, 0, 0)$	$\pm 0.7898325i \quad \pm 1.0304795i \quad \pm 1.1519976i$
$(0.4856721, 0.1025224, -0.4895725, 0, 0, 0)$	$\pm 0.6535438 \quad \pm 1.0863578i \quad \pm 1.1757842i$
$(-0.4856721, -0.1025224, 0.4895725, 0, 0, 0)$	$\pm 0.6535438 \quad \pm 1.0863578i \quad \pm 1.1757842i$
$(0.0934702, 0.4375559, 0.187268, 0, 0, 0)$	$\pm 0.6100958 \quad \pm 0.7595198 \quad \pm 0.9711627i$
$(-0.0934702, -0.4375559, -0.187268, 0, 0, 0)$	$\pm 0.6100958 \quad \pm 0.7595198 \quad \pm 0.9711627i$
$(0.3936921, 0.4008976, 0.0814390, 0, 0, 0)$	$\pm 0.6777331 \quad \pm 0.7625330i \quad \pm 0.8862569i$
$(-0.3936921, -0.4008976, -0.0814390, 0, 0, 0)$	$\pm 0.6777331 \quad \pm 0.7625330i \quad \pm 0.8862569i$
$(-0.4608604, 0.4876500, -0.3909578, 0, 0, 0)$	$\pm 0.7898325i \quad \pm 1.0304795i \quad \pm 1.1519976i$
$(0.4608604, -0.4876500, 0.3909578, 0, 0, 0)$	$\pm 0.7898325i \quad \pm 1.0304795i \quad \pm 1.1519976i$
$(-0.4856721, 0.4895725, -0.1025224, 0, 0, 0)$	$\pm 0.6535438 \quad \pm 1.0863578i \quad \pm 1.1757842i$
$(0.4856721, -0.4895725, 0.1025224, 0, 0, 0)$	$\pm 0.6535438 \quad \pm 1.0863578i \quad \pm 1.1757842i$

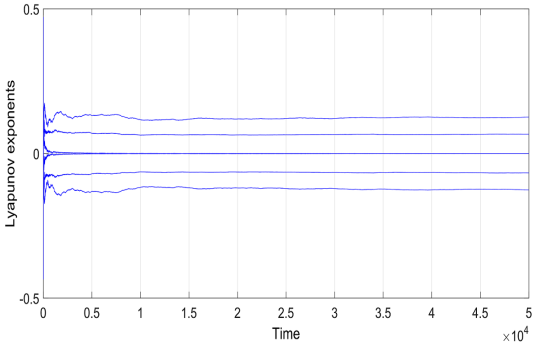

Figure 1. Lyapunov exponents of (2.2).

The Poincaré map of a system is defined by crossings of orbits with one plane [23]. And the evolution of a dynamical system can be studied by using surfaces of section, in which color is used to visualize the fourth dimension [24–29]. Therefore, we consider the projection of 4D space on a 3D subspace, where color is used to indicate the 4th dimension. The (q_1, p_1, p_3, q_2) 4D surface of section is depicted in Figure 2, the location of the consequents is given in the (q_1, p_1, p_3) subspace and are colored according to their q_2 value. The corresponding Poincaré map on the section hyperplane $p_2 = 0$ is shown in Figure 3. Here, initial value is $(0.01, 0.01, 0.01, 0.001, 0.001, 0.001)$. Figure 4 indicates that the Hamiltonian system is sensitive to initial values, where the blue trajectories' initial value is $(0.01, 0.01, 0.01, 0.001, 0.001, 0.001)$, the red trajectories' initial value is $(0.01, 0.01, 0.001, 0.001, 0.001, 0.001)$ and the green trajectories' initial value is $(0, 0, 0, 0.43, 0.09, 0.09)$, respectively.

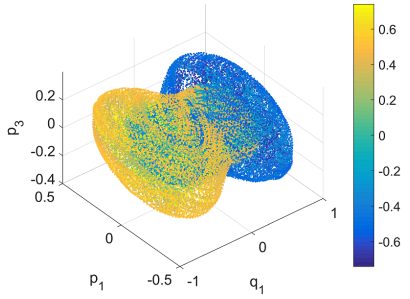

Figure 2. Projection on (q_1, p_1, p_3, q_2).

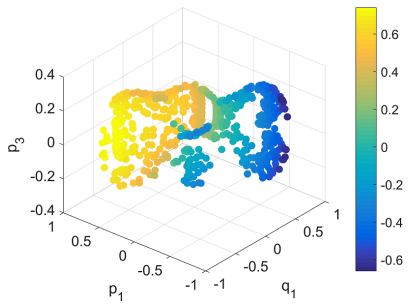

Figure 3. Poincaré map on the section $p_2 + p_3 = 0$.

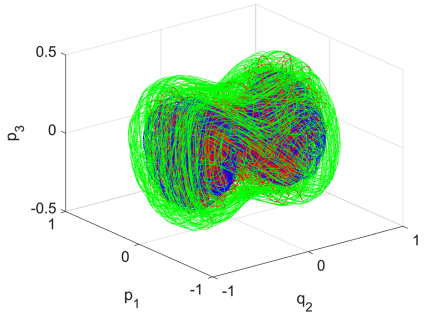

Figure 4. Projections with different initial conditions.

It should be noted that the system has different dynamical characteristics under different initial values, such as initial value is $(0.01, 0.01, 0.001, 0.001, 0.001, 0.001)$, the Lyapunov exponents are:

$$LE_1 \approx 0.123,\ LE_2 \approx 0.038,\ LE_3 \approx 0.000,\ LE_4 \approx -0.000,\ LE_5 \approx -0.038,\ LE_6 \approx -0.123.$$

The spectra of Lyapunov exponents with the initial value is given in Figure 5. The results show that different initial conditions lead to different spectra of Lyapunov exponents and occur different hyperchaotic behaviors. Figure 6 shows the (q_1, p_1, p_3, q_2) 4D surface of section and the location of the consequents is given in the (q_1, p_1, p_3) subspace and are colored according to their q_2 value.

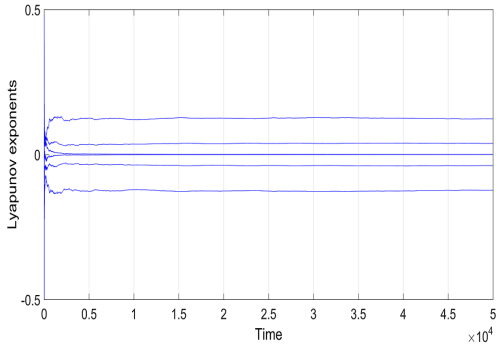

Figure 5. Lyapunov exponents of (2.2).

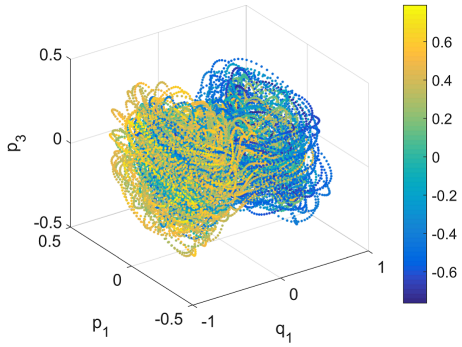

Figure 6. Projection on (q_1, p_1, p_3, q_2).

Obviously, (2.2) is still a Hamiltonian system when the parameters of the Hamiltonian system are all non-positive. There are still many equilibrium points in the system under certain parameters, such as $\eta = -0.2, \theta = -0.5, \beta = -1$. The values of equilibrium points and their corresponding characteristic root results are given in Table 2. In this section, since we mainly focus on the dynamical behaviors of the Hamiltonian system with positive parameters, the detailed analysis of (2.2) with non-positive parameters is omitted.

Table 2. The equilibrium points and their corresponding eigenvalues of system (2.2).

equilibrium points	eigenvalues of Jacobian matrix at these equilibria
$(0, 0, 0, 0, 0, 0)$	$\pm 0.7071067i \quad \pm 0.873812i \quad \pm 0.443228i$
$(0, -0.7071067, 0.7071067, 0, 0, 0)$	$\pm 1.000000 \quad \pm 0.7161559i \quad \pm 1.0260990$
$(0, 0.7071067, -0.7071067, 0, 0, 0)$	$\pm 1.000000 \quad \pm 0.7161559i \quad \pm 1.0260990$
$(-0.5286183, -0.2386217, -0.2386217, 0, 0, 0)$	$\pm 0.6910036 \quad \pm 0.5737411i \quad \pm 0.6544866i$
$(0.5286183, 0.2386217, 0.2386217, 0, 0, 0)$	$\pm 0.6910036 \quad \pm 0.5737411i \quad \pm 0.6544866i$
$(-0.9116707, 0.8459018, 0.8459018, 0, 0, 0)$	$\pm 1.2236845 \quad \pm 1.2832186 \quad \pm 1.4773885$
$(0.9116707, -0.8459018, -0.8459018, 0, 0, 0)$	$\pm 1.22368453 \quad \pm 1.2832186 \quad \pm 1.4773885$

3. The system under constraint conditions

Constraints exist in a wide range of systems, such as fluid particle systems [30], multi-qubit systems [31] and robotic system [32], etc. In this section, we mainly study the hyperchaotic phenomena in system (2.2) under the holonomic constraint condition and nonholonomic constraint condition.

3.1. Holonomic constraint

Assume the constraint on Hamiltonian system (2.2) is

$$q_1^2 + q_2^2 + q_3^2 = L^2. \tag{3.1}$$

Differentiating Eq (3.1) with respect to time, we obtain

$$\phi(\boldsymbol{q}, \boldsymbol{p}) := \boldsymbol{q}\boldsymbol{p}^T = 0, \tag{3.2}$$

where

$$\boldsymbol{q} = (q_1, q_2, q_3), \boldsymbol{p} = (p_1, p_2, p_3).$$

Differentiating Eq (3.2) with respect to time, we have

$$A_p \dot{\boldsymbol{p}}^T = b_{\boldsymbol{p}}, \tag{3.3}$$

where

$$A_{\boldsymbol{p}} = \boldsymbol{q}, b_{\boldsymbol{p}} = -\boldsymbol{p}\boldsymbol{p}^T.$$

The matrix

$$H_{\boldsymbol{pp}}^{-1} = (\tfrac{\partial^2 H}{\partial \boldsymbol{p}^2})^{-1} = \boldsymbol{I}_3.$$

[15] presented a method for getting the explicit equations of constrained Hamiltonian system through the development of the connection between the Lagrangian concept of virtual displacements and Hamiltonian dynamics. By using the three-step approach in [15], the holonomic Hamiltonian system [(2.2), (3.1)] becomes

$$\begin{cases} \dot{\boldsymbol{q}} = \frac{\partial H}{\partial \boldsymbol{p}}, \\ \dot{\boldsymbol{p}} = -\frac{\partial H}{\partial \boldsymbol{q}} + C(\boldsymbol{q},\boldsymbol{p}), \end{cases} \tag{3.4}$$

where

$$C(\boldsymbol{q},\boldsymbol{p}) = (\boldsymbol{I}_3)^{-1}\boldsymbol{q}^T(\boldsymbol{q}\boldsymbol{I}_3{}^{-1}\boldsymbol{q}^T)^{-1}(-\boldsymbol{p}\boldsymbol{p}^T + \boldsymbol{q}\frac{\partial H}{\partial \boldsymbol{q}}).$$

Then,

$$C(\boldsymbol{q},\boldsymbol{p}) = \boldsymbol{I}_3\begin{pmatrix} q_1 \\ q_2 \\ q_3 \end{pmatrix}(q_1^2+q_2^2+q_3^2)^{-1}(b_{\boldsymbol{p}} + A_{\boldsymbol{p}}\frac{\partial H}{\partial \boldsymbol{q}}) = \frac{1}{L^2}\begin{pmatrix} q_1 \\ q_2 \\ q_3 \end{pmatrix}C_1(\boldsymbol{q},\boldsymbol{p}),$$

where

$$C_1(\boldsymbol{q},\boldsymbol{p}) = \beta\, {q_1}^4 + \beta\, {q_2}^4 + \beta\, {q_3}^4 - \eta^2 {q_1}^2 + 2\,\eta\, q_1 q_2 + 2\,\eta\, q_1 q_3 - \theta\, {q_1}^2 - \theta\, {q_2}^2 - \theta\, {q_3}^2 - {p_1}^2 - {p_2}^2 - {p_3}^2.$$

Thus the holonomic Hamiltonian system is transformed into

$$\begin{cases} \dot{\boldsymbol{q}} = \boldsymbol{p}, \\ \dot{p}_1 = \frac{F_1(q_1,q_2,q_3,p_1,p_2,p_3)}{L^2}, \\ \dot{p}_2 = \frac{F_2(q_1,q_2,q_3,p_1,p_2,p_3)}{L^2}, \\ \dot{p}_3 = \frac{F_3(q_1,q_2,q_3,p_1,p_2,p_3)}{L^2}, \end{cases} \tag{3.5}$$

where

$$\begin{aligned} F_1(q_1,q_2,q_3,p_1,p_2,p_3) = {} & -L^2\beta\, {q_1}^3 + \beta\, {q_1}^5 + \beta\, q_1 {q_2}^4 + \beta\, q_1 {q_3}^4 + L^2\eta^2 q_1 - \eta^2 {q_1}^3 - L^2\eta\, q_2 - L^2\eta\, q_3 \\ & + 2\,\eta\, {q_1}^2 q_2 + 2\,\eta\, {q_1}^2 q_3 - {p_1}^2 q_1 - {p_2}^2 q_1 - {p_3}^2 q_1, \\ F_2(q_1,q_2,q_3,p_1,p_2,p_3) = {} & -L^2\beta\, {q_2}^3 + \beta\, {q_1}^4 q_2 + \beta\, {q_2}^5 + \beta\, q_2 {q_3}^4 - \eta^2 {q_1}^2 q_2 - \eta\, q_1 L^2 + 2\,\eta\, q_1 {q_2}^2 + 2\,\eta\, q_1 q_2 q_3 \\ & - {p_1}^2 q_2 - {p_2}^2 q_2 - {p_3}^2 q_2, \\ F_3(q_1,q_2,q_3,p_1,p_2,p_3) = {} & -L^2\beta\, {q_3}^3 + \beta\, {q_1}^4 q_3 + \beta\, {q_2}^4 q_3 + \beta\, {q_3}^5 - \eta^2 {q_1}^2 q_3 - \eta\, q_1 L^2 + 2\,\eta\, q_1 q_2 q_3 + 2\,\eta\, q_1 {q_3}^2 \\ & - {p_1}^2 q_3 - {p_2}^2 q_3 - {p_3}^2 q_3. \end{aligned}$$

Obviously, the system (3.5) is invariant for the coordinate transformation

$$(q_1, q_2, q_3, p_1, p_2, p_3) \to (-q_1, -q_2, -q_3, -p_1, -p_2, -p_3).$$

In order to intuitively reflect the complex dynamical behaviors of the constraint system, we fix the parameters $\beta = 2.5$, $\eta = 1$ and $L = 0.01$. The calculations show that the system (3.5) has six equilibrium points, the values of equilibrium points and their corresponding characteristic root results are given in Table 3.

Table 3. The equilibrium points and their corresponding eigenvalues of system (3.5).

equilibrium points	eigenvalues of Jacobian matrix at these equilibria
$(0.0000000, 0.0070710, -0.0070710, 0, 0, 0)$	$\pm 0.0001581 \quad \pm 0.0141421 \quad \pm 0.0100006i$
$(0.0000000, -0.0070710, 0.0070710, 0, 0, 0)$	$\pm 0.0001581 \quad \pm 0.0141421 \quad \pm 0.0100006i$
$(0.0057735, 0.0057735, 0.0057735, 0, 0, 0)$	$\pm 0.0099991 \quad \pm 0.0141427 \quad \pm 0.0173200$
$(-0.0057735, -0.0057735, -0.0057735, 0, 0, 0)$	$\pm 0.0099991 \quad \pm 0.0141427 \quad \pm 0.0173200$
$(-0.0081648, 0.0040825, 0.0040825, 0, 0, 0)$	$\pm 0.0141421i \quad \pm 0.0173208i \quad \pm 0.0199993i$
$(0.0081648, -0.0040825, -0.0040825, 0, 0, 0)$	$\pm 0.0141421i \quad \pm 0.0173208i \quad \pm 0.0199993i$

Similarly, it indicate that the system (3.5) has unstable manifold and stable manifold at the equilibrium points. The Lyapunov exponents are obtained as follows:

$$LE_1 \approx 0.004, LE_2 \approx 0.001, LE_3 \approx 0.000, LE_4 \approx 0.000, LE_5 \approx -0.004, LE_6 \approx -0.001,$$

the initial value is $(0, 0, 0.01, 0.011, 0.051, 0.051)$. Therefore, the holonomic system (3.5) is hyperchaotic. Figure 7 indicates that the holonomic Hamiltonian system is sensitive to initial values, where the blue trajectories' initial value is $(0, 0, 0.01, 0.011, 0.051, 0.051)$, the magenta trajectories' initial value is $(0, 0.01, 0, 0.011, 0.051, 0.051)$ and the green trajectories' initial value is $(0.01, 0, 0, 0.011, 0.051, 0.051)$, respectively. The (q_3, p_1, p_3, q_2) 4D surface of section of Poincaré section on the section hyperplane $p_2 = 0$ for the first condition is depicted in Figure 8, the location of the consequents is given in the (q_3, p_1, p_3) subspace and are colored according to their q_2 value.

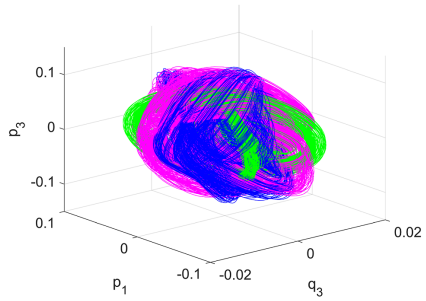

Figure 7. Projections with different initial values.

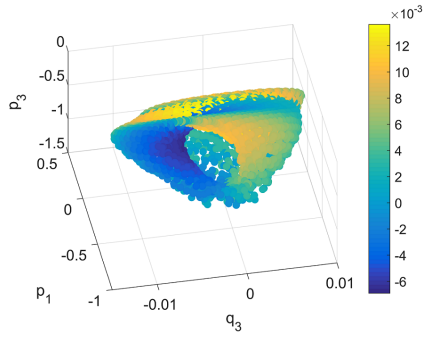

Figure 8. Poincaré map on the section $p_2 = 0$.

3.2. Nonholonomic constraint

Assume the constraint on Hamiltonian system (2.2) is

$$\dot{q}_1 + \dot{q}_2 - q_3 = 0. \tag{3.6}$$

Differentiating Eq (3.6) with respect to time, we have $\ddot{q}_1 + \ddot{q}_2 = \dot{q}_3$, then

$$A_p = (1, 1, 0), b_p = p_3, H_{pp} = I_3.$$

By using the method in [15], the nonholonomic constraint system [(2.2), (3.6)] is equivalent to

$$\begin{cases} \dot{\boldsymbol{q}} = \boldsymbol{p}, \\ \dot{p}_1 = G_1(q_1, q_2, q_3, p_1, p_2, p_3), \\ \dot{p}_2 = G_2(q_1, q_2, q_3, p_1, p_2, p_3), \\ \dot{p}_3 = -\beta {q_3}^3 - \eta q_1 + \theta q_3, \end{cases} \tag{3.7}$$

where

$$G_1(q_1, q_2, q_3, p_1, p_2, p_3) = \tfrac{1}{2}(p_3 + \theta q_1 - \theta q_2 + \eta q_1 - \eta q_2 - \eta q_3 - \beta {q_1}^3 + \beta {q_2}^3 + \eta^2 q_1),$$

$$G_2(q_1, q_2, q_3, p_1, p_2, p_3) = \tfrac{1}{2}(p_3 - \theta q_1 + \theta q_2 - \eta q_1 + \eta q_2 + \eta q_3 + \beta {q_1}^3 - \beta {q_2}^3 - \eta^2 q_1).$$

Similarly, we fix the parameters $\theta = 0.5, \beta = 2.5, \eta = 0.1$, the nonholonomic system (3.7) has three unstable equilibrium point

$$(0, 0, 0, 0, 0, 0), \quad (0, 0.4898979, 0, 0, 0, 0), \quad (0, -0.4898979, 0, 0, 0, 0),$$

the corresponding eigenvalues of Jacobian matrix of (3.7) at these equilibria are

$$0,\ 0.1030839,\ 0.6312678,\ 0.7933172,\ -0.7156897,\ -0.8119793;$$
$$0,\ -0.7937423,\ 0.4699607 \pm 0.0358103i,\ -0.0730895 \pm .5787367i;$$
$$0,\ -0.7937423,\ 0.4699607 \pm 0.0358103i,\ -0.0730895 \pm .5787367i.$$

The Lyapunov exponents are

$$LE_1 \approx 0.002, LE_2 \approx 0.001, LE_3 \approx 0.000, LE_4 \approx -0.000, LE_5 \approx -0.001, LE_6 \approx -0.003,$$

here initial value is $(0, 0.02, 0.02, 0.01, 0.01, 0.2)$. Thus, the nonholonomic constrained Hamiltonian system is hyperchaotic. Figure 9 shows the (q_1, q_3, p_1, p_2) 4D surface of section and the location of the consequents is given in the (q_1, q_3, p_1) subspace and are colored according to their p_2 value. The corresponding Poincaré map on the section hyperplane $p_3 = 0$ is given in Figure 10.

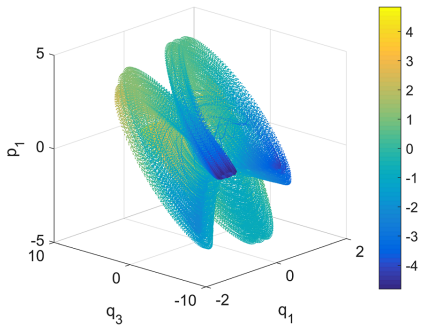

Figure 9. Projection on (q_1, q_3, p_1, p_2).

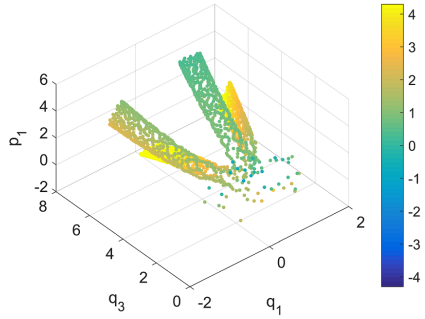

Figure 10. Poincaré map on the section $p_3 = 0$.

4. Hyperchaos control

From the above discussion, we can see that the constraints (3.1) and (3.6) have changed the status of the hyperchaotic system. It indicates that the hyperchaotic system can be generated by introducing constraint into higher-dimension Hamiltonian system. In some cases, the hyperchaotic behaviors will cause serious harm, for example, may lead to catastrophic voltage collapse or even blackout in actual power system [33], thus, these hyperchaotic systems need to be controlled by appropriated methods. In this section, we will investigate the control problem of the hyperchaotic system. Chaos control has been widely concerned by scholars, and many valuable chaotic controller have been designed, such as optimal control [34, 35], impulse control [36], feedback control [37], etc. To achieve hyperchaos control, the linear feedback control [37] is used to suppress hyperchaos to stable equilibrium. Suppose that the controlled system is the following form:

$$\begin{cases} \dot{\boldsymbol{q}} = \boldsymbol{p} + u\boldsymbol{q}, \\ \dot{p}_1 = -\beta q_1^3 + (\eta^2 + \theta)q_1 - \eta(q_2 + q_3) + up_1, \\ \dot{p}_2 = -\beta q_2^3 + \theta q_2 - \eta q_1 + up_2, \\ \dot{p}_3 = -\beta q_3^3 + \theta q_3 - \eta q_1 + up_3, \end{cases} \tag{4.1}$$

where u is feedback coefficient. We select the same values of the parameters in Section 2, the Jacobian matrix of (4.1) is

$$J_c = \begin{bmatrix} u & 0 & 0 & 1 & 0 & 0 \\ 0 & u & 0 & 0 & 1 & 0 \\ 0 & 0 & u & 0 & 0 & 1 \\ -7.5\,{q_1}^2 + 0.51 & -0.1 & -0.1 & u & 0 & 0 \\ -0.1 & -7.5\,{q_2}^2 + 0.5 & 0 & 0 & u & 0 \\ -0.1 & 0 & -7.5\,{q_3}^2 + 0.5 & 0 & 0 & u \end{bmatrix}.$$

When $u = -1$, there is only one zero-equilibrium point $(0, 0, 0, 0, 0, 0)$ in the system (4.1). By computations, the eigenvalues of J_c is as follows:

$$-1.707,\ -0.293,\ -1.602,\ -1.804,\ -0.397,\ -0.959.$$

Therefore, the controlled hyperchaotic system (4.1) is asymptotically stable at equilibrium

$(0, 0, 0, 0, 0, 0)$. The behaviors of the state $q_1, q_2, q_3, p_1, p_2, p_3$ of (2.2) and (4.1) with time are shown in Figures 11 and 12, respectively. Here, the horizontal coordinate data denote time, initial value is $(0.01, 0.01, 0.01, 0.001, 0.001, 0.001)$.

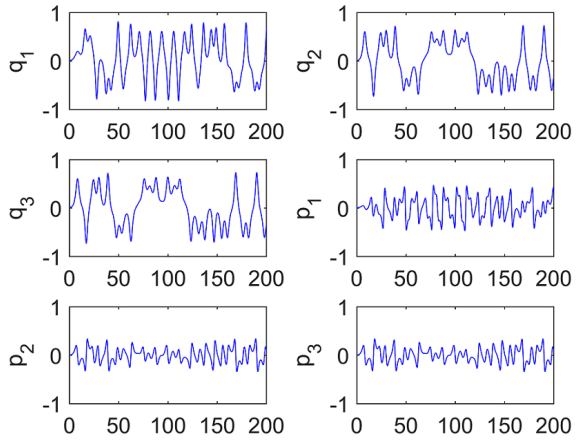

Figure 11. Time series of (2.2).

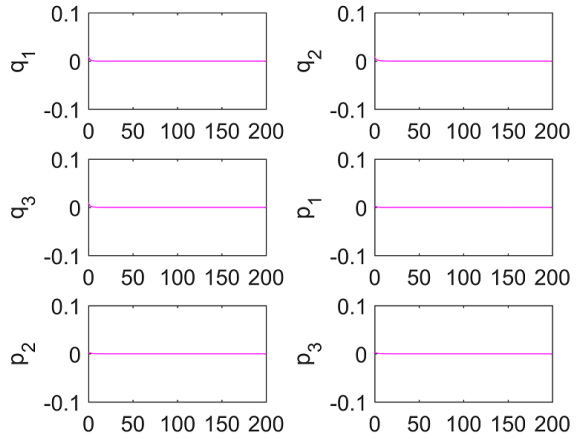

Figure 12. Time series of (4.1).

It should be noted that the linear feedback control method is also applicable in system (3.5). In this case, the controlled system is as follows:

$$\begin{cases} \dot{\boldsymbol{q}} = \boldsymbol{p} + k\boldsymbol{q}, \\ \dot{p}_1 = \frac{F_1(q_1,q_2,q_3,p_1,p_2,p_3)}{L^2} + kp_1, \\ \dot{p}_2 = \frac{F_2(q_1,q_2,q_3,p_1,p_2,p_3)}{L^2} + kp_2, \\ \dot{p}_3 = \frac{F_3(q_1,q_2,q_3,p_1,p_2,p_3)}{L^2} + kp_3. \end{cases} \tag{4.2}$$

Similarly, we obtain the unique asymptotic stable equilibrium point $\boldsymbol{E}_1(0, 0, 0, 0, 0, 0)$, the corresponding eigenvalues at $\boldsymbol{E}_1$ is as follows:

$$-5.01, \quad -4.99, \quad -5, \quad -5, \quad -5, \quad -5,$$

here $k = -5$. The controlled hyperchaotic system (4.2) is asymptotically stable at $\boldsymbol{E}_1$.

The behaviors of the state $q_1, q_2, q_3, p_1, p_2, p_3$ of (3.5) and (4.2) with time are shown in Figures 13 and 14, respectively. Here, the horizontal coordinate data denote time, initial value is $(0, 0, 0.01, 0.011, 0.051, 0.051)$. In conclusion, the hyperchaos control of the hyperchaotic system (2.2) and system (3.5) can be achieved by selecting appropriate feedback coefficients.

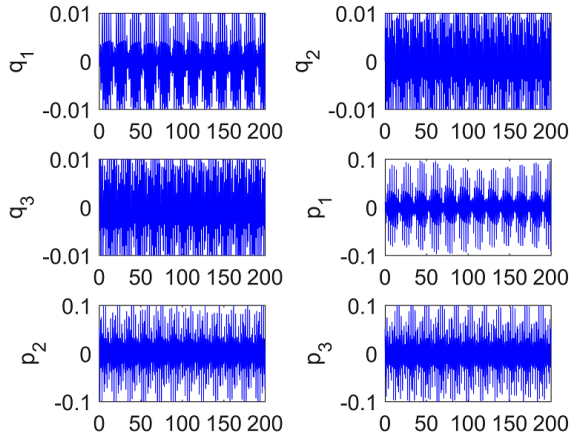

Figure 13. Time series of (3.5).

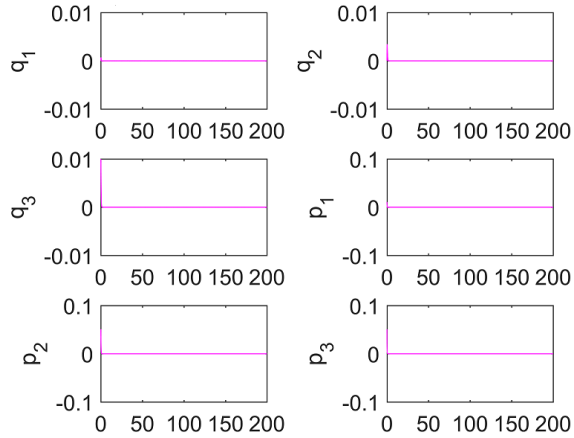

Figure 14. Time series of (4.2).

5. Conclusions

In this paper, a new hyperchaotic Hamiltonian system is formulated and analysis the complex dynamic behaviors including the multi-equilibrium points their characteristics, Poincaré section, Lyapunov exponents. The explicit equations of the Hamiltonian system under holonomic constraint and nonholonomic constraint are obtained. The results show that the constrained systems have different dynamic behaviors from the unconstrained system and the new hyperchaotic systems are generated by introducing holonomic constraint and nonholonomic constraint. Finally, the hyperchaos control is achieved by using linear feedback which suppress hyperchaotic system to asymptotic stable zero-equilibrium.

Acknowledgments

Project supported by the Doctoral Scientific Research Foundation of Hanshan Normal University (No. QD202130).

Conflict of interest

The authors declare that they have no competing interests in this paper.

References

1. G. Franzese, H. E. Stanley, Liquid-liquid critical point in a Hamiltonian model for water: Analytic solution, *J. Phys.: Condens. Matter*, **14** (2002), 2201–2209. https://doi.org/10.1088/0953-8984/14/9/309
2. T. Igata, T. Koike, H. Ishihara, Constants of motion for constrained Hamiltonian systems: A particle around a charged rotating black hole, *Phys. Rev. D*, **83** (2010), 065027. https://doi.org/10.1103/PhysRevD.83.065027
3. D. G. C. Mckeon, Hamiltonian formulation of the Freedman-Townsend model of massive vector mesons, *Can. J. Phys.*, **69** (2011), 569–572. https://doi.org/10.1139/p91-094
4. B. B. Xu, D. Y. Chen, H. Zhang, F. F. Wang, X. G. Zhang, Y. H. Wu, Hamiltonian model and dynamic analyses for a hydro-turbine governing system with fractional item and time-lag, *Commun. Nonlinear Sci.*, **47** (2017), 35–47. https://doi.org/10.1016/j.cnsns.2016.11.006
5. J. L. Bona, X. Carvajal, M. Panthee, M. Scialom, Higher-Order Hamiltonian model for unidirectional water waves, *J. Nonlinear Sci.*, **28** (2018), 543–577. https://doi.org/10.1007/s00332-017-9417-y
6. G. Contopoulos, *Order and chaos in dynamical astronomy*, Berlin Heidelberg: Springer, 2004.
7. T. Bountis, H. Skokos, *Complex Hamiltonian dynamics*, Berlin Heidelberg: Springer, 2012.
8. H. Y. Jia, W. X. Shi, L. Wang, G. Y. Qi, Energy analysis of Sprott-A system and generation of a new Hamiltonian conservative chaotic system with coexisting hidden attractors, *Chaos Soliton. Fract.*, **133** (2020), 109635. https://doi.org/10.1016/j.chaos.2020.109635
9. J. C. Sprott, Some simple chaotic flows, *Phys. Rev. E*, **50** (1994), R647–R650. https://doi.org/10.1103/PhysRevE.50.R647
10. D. Jánosi, T. Tél, Chaos in Hamiltonian systems subjected to parameter drift, *Chaos*, **29** (2019), 121105. https://doi.org/10.1063/1.5139717
11. F. Ginelli, K. A. Takeuchi, H. Chaté, A. Politi, A. Torcini, Chaos in the Hamiltonian mean-field model. *Phys. Rev. E*, **84** (2011), 066211. https://doi.org/10.1103/PhysRevE.84.066211
12. E. Z. Dong, M. F. Yuan, S. Z. Du, Z. Q. Chen, A new class of Hamiltonian conservative chaotic systems with multistability and design of pseudo-random number generator, *Appl. Math. Model.*, **73** (2019), 40–71. https://doi.org/10.1016/j.apm.2019.03.037

13. D. Martínez-Del-Río, D. del-Castillo-Negrete, A. Olvera, R. Calleja, Self-consistent chaotic transport in a high-dimensional mean-field Hamiltonian map model. *Qual. Theory Dyn. Syst.*, **14** (2015), 313–335. https://doi.org/10.1007/s12346-015-0168-6

14. L. Crane, Hyperchaos could help us build better quantum computers, *New Sci.*, **249** (2021), 15. https://doi.org/10.1016/S0262-4079(21)00136-6

15. F. E. Udwadia, Constrained motion of Hamiltonian systems, *Nonlinear Dyn.*, **84** (2016), 1135–1145. https://doi.org/10.1007/s11071-015-2558-3

16. C. Skokos, On the stability of periodic orbits of high dimensional autonomous Hamiltonian systems, *Physica D*, **159** (2001), 155–179. https://doi.org/10.1016/S0167-2789(01)00347-5

17. P. Gaspard, M. B. Briggs, M. K. Francis, J. V. Sengers, R. W. Gammon, J. R. Dorfman, et al., Experimental evidence for microscopic chaos, *Nature*, **394** (1998), 865–868. https://doi.org/10.1038/29721

18. G. Benettin, L. Galgani, A. Giorgilli, J. M. Strelcyn, Lyapunov characteristic exponents for smooth dynamical systems and for hamiltonian systems; A method for computing all of them. Part 2: Numerical application, *Meccanica*, **15** (1980), 21–30. https://doi.org/10.1007/BF02128237

19. C. Skokos, The Lyapunov characteristic exponents and their computation, In: *Dynamics of small solar system bodies and exoplanets*, Berlin Heidelberg: Springer, 2010. https://doi.org/10.1007/978-3-642-04458-8_2

20. A. Wolf, J. B. Swift, H. L. Swinney, J. A. Vastano, Determining Lyapunov exponents from a time series, *Physica D*, **16** (1985), 285–317. https://doi.org/10.1016/0167-2789(85)90011-9

21. J. A. Vastano, E. J. Kostelich, Comparison of algorithms for determining Lyapunov exponents from experimental data, In: *Dimensions and entropies in chaotic systems*, Berlin Heidelberg: Springer, 1986. https://doi.org/10.1007/978-3-642-71001-8_13

22. O. E. Rössler, An equation for continuous chaos, *Phys. Lett. A*, **57** (1976), 397–398. https://doi.org/10.1016/0375-9601(76)90101-8

23. A. J. Lichtenberg, M. A. Lieberman, Regular and chaotic dynamics, New York: Springer, 1992. https://doi.org/10.1007/978-1-4757-2184-3

24. P. A. Patsis, L. Zachilas, Using color and rotation for visualizing four-dimensional Poincare cross-sections: With applications to the orbital behavior of a three-dimensional hamiltonian system, *Int. J. Bifurcat. Chaos*, **4** (1994), 1399–1424. https://doi.org/10.1142/S021812749400112X

25. M. Katsanikas, P. A. Patsis, The structure of invariant tori in a 3D galactic potential, *Int. J. Bifurcat. Chaos*, **21** (2011), 467–496. https://doi.org/10.1142/S0218127411028520

26. M. Katsanikas, P. A. Patsis, G. Contopoulos, Instabilities and stickiness in a 3D rotating galactic potential, *Int. J. Bifurcat. Chaos*, **23** (2013), 1330005. https://doi.org/10.1142/S021812741330005X

27. S. Lange, M. Richter, F. Onken, A. Bäcker, Global structure of regular tori in a generic 4D symplectic map, *Chaos*, **24** (2014), 024409. https://doi.org/10.1063/1.4882163

28. F. Onken, S. Lange, R. Ketzmerick, A. Bäcker, Bifurcations of families of 1D-tori in 4D symplectic maps, *Chaos*, **26** (2016), 063124. https://doi.org/10.1063/1.4954024

29. M. Richter, S. Lange, A. Bäcker, R. Ketzmerick, Visualization and comparison of classical structures and quantum states of four-dimensional maps, *Phys. Rev. E*, **89** (2014), 022902. https://doi.org/10.1103/PhysRevE.89.022902

30. Z. Chen, L. G. Gibilaro, N. Jand, Particle packing constraints in fluid-particle system simulation, *Comput. Chem. Eng.*, **27** (2003), 681–687. https://doi.org/10.1016/S0098-1354(02)00258-2

31. J. S. Kim, Generalized entanglement constraints in multi-qubit systems in terms of Tsallis entropy, *Ann. Phys.*, **373** (2016), 197–206. https://doi.org/10.1016/j.aop.2016.07.021

32. C. Behn, K. Siedler, Adaptive PID-tracking control of muscle-like actuated compliant robotic systems with input constraints, *Appl. Math. Model.*, **67** (2019), 9–21. https://doi.org/10.1016/j.apm.2018.10.012

33. J. B. Wang, L. Liu, C. X. Liu, Sliding mode control with mismatched disturbance observer for chaotic oscillation in a seven-dimensional power system model, *Int. T. Electr. Energy*, **30** (2020), e12583. https://doi.org/10.1002/2050-7038.12583

34. H. J. Peng, X. W. Wang, B. Y. Shi, Z. Sheng, B. S. Chen, Stabilizing constrained chaotic system using a symplectic psuedospectral method, *Commun. Nonlinear Sci.*, **56** (2018), 77–92. https://doi.org/10.1016/j.cnsns.2017.07.028

35. X. W. Wang, J. Liu, H. J. Peng, L. C. Gao, J. Fottner, P. L. Liu, Input-constrained chaos synchronization of horizontal platform systems via a model predictive controller, *P. I. Mech. Eng. C-J. Mec.*, **235** (2021), 4862–4872. https://doi.org/10.1177/0954406220979005

36. M. F. Danca, M. Feckan, N. Kuznetsov, Chaos control in the fractional order logistic map via impulses, *Nonlinear Dyn.*, **98** (2019), 1219–1230. https://doi.org/10.1007/s11071-019-05257-2

37. F. Dou, J. Sun, W. Duan, K. Lü, Controlling hyperchaos in the new hyperchaotic system. *Commun. Nonlinear Sci.*, **14** (2009), 552–559. https://doi.org/10.1016/j.cnsns.2007.10.009

AIMS Press